The Astrophysical Journal, 707:L148–L152, 2009 December 20 doi:10.1088/0004-637X/707/2/L148

THE DISCOVERY OF A PULSAR WIND NEBULA AROUND THE MAGNETAR CANDIDATE AXP 1E1547.0-5408

Jacco Vink[1] and Aya Bamba[2,3]
[1] Astronomical Institute, Utrecht University, P.O. Box 80000, 3508TA Utrecht, The Netherlands; j.vink@astro.uu.nl
[2] Dublin Institute for Advanced Studies, 5 Merrion Square, Dublin 2, Ireland
[3] ISAS/JAXA Department of High Energy Astrophysics, 3-1-1 Yoshinodai, Sagamihara, Kanagawa 229-8510, Japan
Received 2009 September 21; accepted 2009 November 17; published 2009 December 4

ABSTRACT

We report the detection of extended emission around the anomalous X-ray pulsar 1E1547.0-5408 using archival data of the *Chandra* X-ray satellite. The extended emission consists of an inner part, with an extent of 45″, and an outer part with an outer radius of 2.′9, which coincides with a supernova remnant shell previously detected in the radio. We argue that the extended emission in the inner part is the result of a pulsar wind nebula (PWN), which would be the first detected PWN around a magnetar candidate. Its ratio of X-ray luminosity versus pulsar spin-down power is comparable to that of other young PWNe, but its X-ray spectrum is steeper than most PWNe. We discuss the importance of this source in the context of magnetar evolution.

Key words: stars: magnetic fields – stars: neutron

1. INTRODUCTION

Among the various types of neutron stars, soft gamma-ray repeaters (SGRs) and anomalous X-ray pulsars (AXPs) stand out by their extreme bursting behavior, high X-ray luminosity, and long rotation periods of 2–12 s (see Woods & Thompson 2006; Mereghetti 2008, for reviews). They are now widely recognized as magnetars, neutron stars with extreme surface magnetic fields of 10^{14}–10^{15} G, well above the quantum critical magnetic field of $B_{\rm QED} = 4.4 \times 10^{13}$ G. The X-ray luminosity and bursts of magnetars are thought to be powered by the decaying magnetic field. Despite their extreme energy output, the particle acceleration properties of magnetars are not well known.

Here we report the detection of a pulsar wind nebula (PWN) around AXP 1E1547.0-5408. We show that the nebula's brightness is comparable to that of normal pulsars with the same rotational energy loss rate. This suggests that the nebula is powered by rotational energy loss, rather than by the magnetar's magnetic field.

1.1. 1E1547.0-5408

1E1547.0-5408 (Lamb & Markert 1981) is an X-ray source that was only recently recognized to belong to the class of magnetars (Gelfand & Gaensler 2007), a name we adopt here to refer to both SGRs and AXPs. With its rotation period of $P = 2.1$ s (Camilo et al. 2007), it is the most rapidly spinning magnetar known. Its period derivative is $\dot{P} = 2.3 \times 10^{-11}$, which, combined with the period, implies a surface magnetic field of $B_{\rm dipole} = 3.2 \times 10^{19}\sqrt{P\dot{P}} = 2.2 \times 10^{14}$ G, and a rotational energy loss rate of $\dot{E} = 1.0 \times 10^{35}$ erg s^{-1}, the highest among AXPs and SGRs. 1E1547.0-5408 is also a transient radio source (Camilo et al. 2007), a characteristic shared with only one other magnetar, AXP XTE J1810-197 (Camilo et al. 2006). Very recently, 1E1547.0-5408 went through a period of major bursting activity (Krimm et al. 2008a, 2008b; Gronwall et al. 2008), confirming its status as a magnetar.

1E1547.0-5408 is located inside a supernova remnant (SNR) shell, G327.24-0.13, detected with the Molongo Radio Observatory (Gelfand & Gaensler 2007). Although the spin-down rates of most AXPs/SGRs imply that they are young sources (typically $<10^5$ yr), only a few of them are associated with SNRs (Gaensler 2004). These SNRs may hold important clues about the supernovae that created the magnetars. In particular, the energy of the remnants indicates that the supernovae creating magnetars are not more powerful than ordinary supernovae (Vink & Kuiper 2006). This poses a challenge to the scenario in which magnetars are born with extremely high initial spin periods (Duncan & Thompson 1992), in which case $\sim 10^{52}$ erg rotational energy is likely to be transferred to the supernova ejecta. Nevertheless, this scenario cannot be completely excluded, because the distances used by Vink & Kuiper (2006) have been disputed (Durant & van Kerkwijk 2006).

A major obstacle in determining the initial spin periods of AXPs/SGRs is that they spin down rapidly and often irregularly (e.g., Gavriil et al. 2004; Esposito et al. 2009). It is, therefore, difficult to determine whether they were born with periods close to their current spin periods, or with periods comparable to, or even shorter than ordinary pulsars. Provided that the nebula around 1E1547.0-5408 is indeed powered by rotational energy loss, its properties may help to clarify its rotational history, as PWNe contain most of the initial rotational energy lost over the lifetime of the pulsar (e.g., Pacini & Salvati 1973).

In the following section, we report on the details of the detection of extended emission around 1E1547.0-5408, both based on imaging (Section 2.2) and on spectral analysis (Section 2.3). In Section 2.4, we argue that the extended source is most likely a PWN, and not a dust-scattering halo. In the final section, we discuss the implications of the presence of a PWN around 1E1547.0-5408.

2. DATA ANALYSIS AND RESULTS

2.1. Data Selection

In order to find a potential X-ray counterpart to the radio shell of G327.24-0.13, we analyzed archival *Chandra* and *XMM-Newton* data. During this search, we found a faint, but distinct, extended X-ray source, centered on the magnetar. Not all archival data were suitable for our analysis, since several *Chandra* observations were taken in continuous clocking mode,

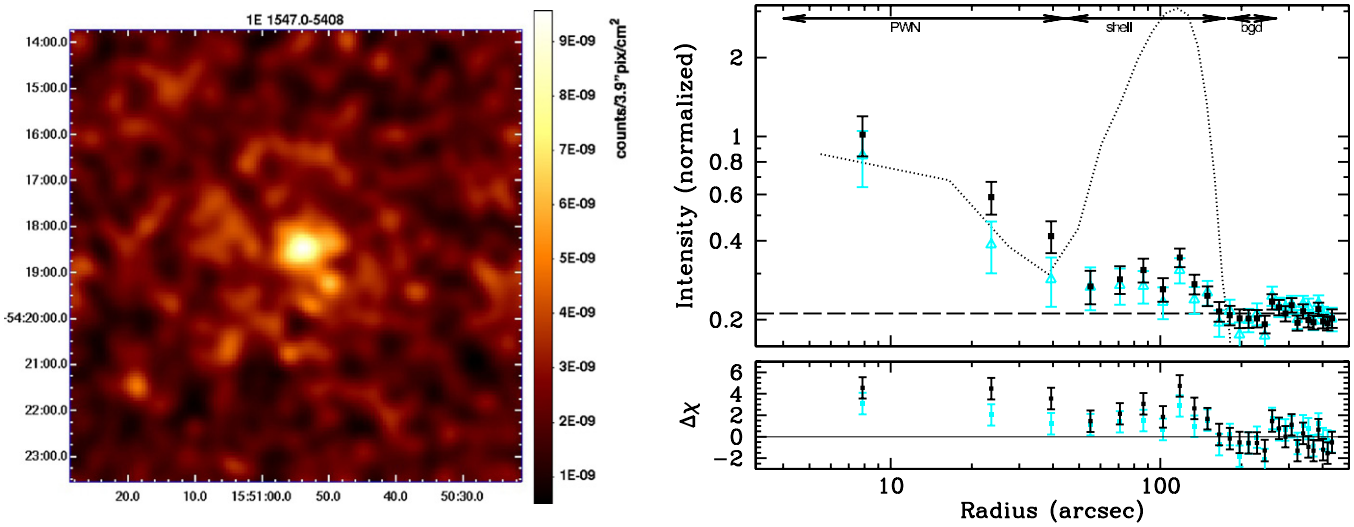

Figure 1. Left:a *Chandra* ACIS-I image of the diffuse emission surrounding 1E1547.0-5408 in the energy range 1.5–7 keV. Several point sources, including 1E1547.0-5408, were removed, and the image was then smoothed with a kernel of $\sigma = 11\farcs8$ (24 pixels). Right: the radial brightness profile in the 1.5–7 keV band (black squares) and radio (dotted line, based on the SUMMS survey; Bock et al. 1999). We have normalized the radio profile such that the central enhancement coincides with extended emission in X-rays. The X-ray background intensity is indicated by the dashed line, and the spectral extraction regions for the PWN, shell, and background (bgd) by two-sided arrows. With cyan triangles we also indicate the profile in the 3–7 keV range.

which does not allow for imaging. This leaves only the 9.6 ks long observation on 2006 July 1, with the ACIS-I detector, as a suitable observation for extended source analysis. Several *XMM-Newton* observations are present in the archive, but the point-spread function (PSF) of *XMM-Newton* is much broader (∼6″ FWHM, with extended broad wings) than that of *Chandra* (∼0.″5 FWHM). Therefore, the *Chandra* data, although poor in statistics, provide a more convincing case for the presence of an extended source. However, we note that the *XMM-Newton* data are consistent with the results presented here.

2.2. Imaging

We performed the analysis of the *Chandra* data using the standard software (CIAO v4.1) to make exposure corrected images, and extract spectra of the magnetar, the extended emission, and the region of the radio shell that was found by Gelfand & Gaensler (2007). The extended source is weak, and can only be seen after significantly smoothing the images. However, the advantage of the small PSF of *Chandra* is that point sources can be effectively removed before smoothing. Apart from X-ray emission within 4″ of the position of 1E1547.0-5408 also other faint point sources in the field were removed, two of which were located in the region of the radio shell.[4] The resulting 1.5–7 keV image is shown in Figure 1 (left). We chose for this energy range, because below 1.5 keV there is hardly any emission to be expected due to the large absorption column (cf, Figure 2 in Gelfand & Gaensler 2007). The image is noisy, but extended emission centered on 1E1547.0-5408 can be seen. This source is surrounded by a faint shell.

The radial X-ray brightness profile makes the structure even more clear (Figure 1 right). We include in this figure the radio intensity profile at 843 MHz as obtained from the Sydney University Molonglo Sky Survey (Bock et al. 1999; Gelfand & Gaensler 2007). We also show the profile using the hardest photons only, 3–7 keV, as this lowers the potential contribution of dust-scattered X-ray emission from 1E1547.0-5408 (see Section 2.4). The profile clearly shows the presence of an extended emission component that falls off with radius and disappears at $r \approx 45''$. Further outward there is a small enhancement out to $r \approx 150''$, which coincides with the radio shell. Also the radio map gives a hint of centrally enhanced emission with an approximate flux density of ∼0.008 Jy at 843 MHz and a radial profile similar to that in X-rays, but with a different brightness ratio between shell and central emission.

The radial brightness profiles allow us to make an estimate of the statistical detection significances. Fitting the first three bins, labeled PWN, with a flat background model results in $\chi^2/\mathrm{dof} = 55.0/3$, corresponding to a 6.9σ detection. In the 3–7 keV band, this reduces to $\chi^2/\mathrm{dof} = 15.3/3$, still a 3.2σ detection. For the radio shell, the numbers are $\chi^2/\mathrm{dof} = 58.6/7$ (6σ) and $\chi^2/\mathrm{dof} = 18.1/7$ (2.5σ), respectively.

2.3. Spectral Analysis

We extracted X-ray spectra of three regions, using a radius of $r = 0\farcs74$ to isolate the spectrum of 1E1547.0-5408 (corresponding to 80% encircled energy); an annulus with an inner radius of 4″ and an outer radius of 45″ for the extended source; and an annulus between 45″ and 174″ for the X-ray counterpart of the radio shell. The inner radius for the extended source guarantees that only ∼5% of the point source contributes to the emission of the extended source, due to the scattering wings of the *Chandra* PSF.[5] Given that the flux of 1E1547.0-5408 appears to be about twice as large as that of the extended source (Table 1), we expect a ∼10% contamination of the extended source from the AXP, due to the wings of the PSF. The background spectrum of the extended source and the shell was obtained from an annulus centered on the AXP with $180'' < r < 272''$. The background spectrum for the AXP was obtained from an annulus with $4'' < r < 20''$, i.e., we treated the extended region as a source of background for the point source.

[4] Their J2000 positions are $\alpha = 15^{\mathrm{h}}51^{\mathrm{m}}07\fs7$, $\delta = -54^\circ19'26\farcs0$, and $\alpha = 15^{\mathrm{h}}50^{\mathrm{m}}34\fs8$, $\delta = -54^\circ19'25\farcs9$, respectively.

[5] The *Chandra* Proposers' Observatory Guide V11.0 Figure 4.20 shows that 95% of the photons with energies of 1.5 keV fall within 2″ of the source position.

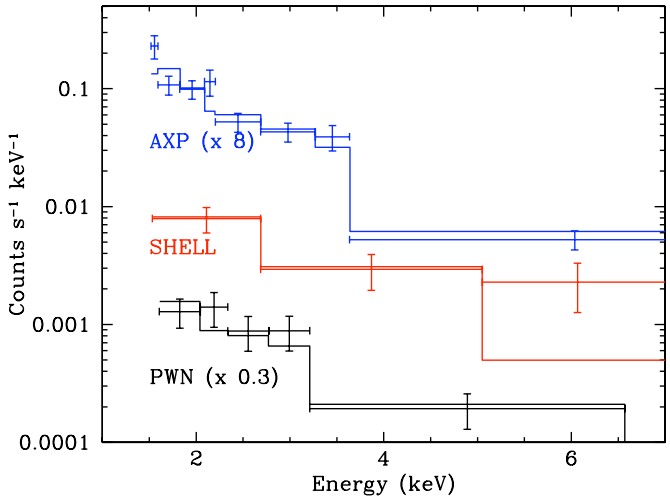

Figure 2. *Chandra* X-ray spectra of the PWN, the SNR shell, and 1E1547.0-5408. The count rates of 1E1547.0-5408 and the PWN have been multiplied by the factors indicated for reasons of clarity. The rebinning was done for display purposes. No rebinning was necessary for the fitting itself as the statistic described in Cash (1979) was used.

Table 1
Spectral Fit Parameters[a]

Component	Flux (2–10 keV) (10^{-13} erg s^{-1}cm^{-2})		Spectral Index
	Absorbed[b]	Unabsorbed	
AXP	2.4 ± 0.3	3.8 ± 0.4	−3.8 ± 0.1
Extended source	1.0 ± 0.3	1.5 ± 0.3	−3.4 ± 0.4
Shell	2.3 ± 0.7	3.5 ± 0.7	−3.3 ± 0.8

Notes.
[a] Based on joint fits of the spectra in the 1.5–7 keV range using the *xspec* v11 package, and employing the *C*-statistic, (Cash 1979). The overall statistic for the joint fit was $C = 74.5$ for 72 bins. Excluding the PWN model fit resulted in $\Delta C = 125$ (11σ), and excluding the shell model resulted in $\Delta C = 110$ (6σ).
[b] The best-fit absorption column was $N_{\rm H} = (2.75 \pm 0.25) \times 10^{22}$ cm^{-2}, using the *tbabs* absorption model (Wilms et al. 2000).

We fitted these data with power-law spectra with a Galactic absorption component. For our analysis, we also investigated an additional blackbody component for the point source, and a non-equilibrium ionization thin plasma model for the radio shell. However, this did not improve the fits. Note that for the *XMM-Newton* data including a blackbody for the point source did improve the fit (Gelfand & Gaensler 2007), but the *XMM-Newton* data have better statistics concerning the spectrum of the point source. According to Gelfand & Gaensler (2007), the best spectrum of the AXP is a combination of a soft power law with the index −3.7 plus a blackbody component with $kT = 0.43$ keV. The *Chandra* data agree with this in the sense that we also find a steep power law. The resulting spectra are shown in Figure 2, and the best-fit parameters are listed in the Table 1.

2.4. A Pulsar Wind Nebula or a Dust-scattering Halo?

The spatial morphology and the spectral characteristics of the extended source have all the characteristics of a PWN created by 1E1547.0-5408, but we need to exclude the possibility that the extended emission could be caused by a dust-scattering halo (e.g., Predehl & Schmitt 1995). Indeed, dust scattering is not absent as indicated by the recent detections of evolving dust-scattering haloes after some major outbursts of 1E1547.0-5408 (Tiengo et al. 2009). However, in the situation investigated here a dust-scattering halo is unlikely to dominate the emission above 3 keV, with a most likely flux contribution to the emission within 45″ of 6%–11%.

Table 2
Expected Dust Scattering Contributions[a]

$\tau_{\rm sca}$ (1 keV)	β[b]	$F_{\rm halo}/F_{\rm obs}$ (1.5 keV)	$F_{\rm halo}/F_{\rm obs}$ (3 keV)	$\Delta\Gamma$
1.5	0	13%	6%	−0.4
1.5	1	25%	11%	−0.5
3.0	0	37%	13%	−0.9
3.0	1	73%	25%	−0.9

Notes.
[a] Prediction based on Equation (19) of Draine (2003).
[b] $\beta = 0$ corresponds to uniformly distributed gas, $\beta = 1$ has three-fourths of the dust at a distance greater than 50% of the total distance (Draine 2003).

Our estimate is based on the relation between the dust-scattering optical depth $\tau_{\rm sca}$ at 1 keV and the absorption column as found by Predehl & Schmitt (1995). For $N_{\rm H} = 3 \times 10^{22}$ cm^{-2} (Table 1 and Gelfand & Gaensler 2007), this gives $\tau_{\rm sca} = 1.5$ at 1 keV, corresponding to $\tau_{\rm sca} = 0.17$ at 3 keV, because the dust-scattering cross section is proportional to E^{-2}. The values of $\tau_{\rm sca}$ can be related to the fractional halo intensity, $I_{\rm frac}$ (Predehl & Schmitt 1995). At 3 keV, this gives $I_{\rm frac} = 15\%$, but most of the halo flux will be outside the spectral extraction radius of 45″. To estimate the fraction within 45″, we use the semi-analytic approximation of Draine (2003), which employs a parameter β to account for gradients in the dust distribution; with $\beta = -1(1)$ corresponding to a dust distribution skewed in distance toward the observer (source), $\beta = 0$ to a uniform distribution. Table 2 lists the potential dust halo contributions to the extended source, which indicates a modest contribution of 11% even for $\beta = 1$.

Draine (2003) discussed the possibility that the relation $N_{\rm H}$ versus $\tau_{\rm sca}$ relation of Predehl & Schmitt (1995) underestimates $\tau_{\rm sca}$ due to the neglect of small angle scattering. For that reason, we also provide in Table 2 values for the expected dust halo contributions for $\tau_{\rm sca} = 3.0$. In that case, the dust halo becomes more substantial, but at 3 keV, with 25% for $\beta = 1$, it still not dominant. Note that the model by Draine (2003) seems to overestimate dust halo scattering: apart from its discrepancy with the results of Predehl & Schmitt (1995), also a recent *Chandra* observation of GX13+1 shows that this model gives a poor fit to the data and underestimates the absorption column (Smith 2008), and overestimates the fraction of small angle scattering. This suggest that the 25% contribution at 3 keV is too conservative, and an <11% seems likely. Moreover, adopting $\tau_{\rm sca} = 3.0$ predicts a steepening of the halo spectrum within 45″ with respect to the source spectrum of $\Delta\Gamma = -0.9$, whereas the actual spectrum of the extended source is flatter than that of the AXP by $\Delta\Gamma = 0.4 \pm 0.5$ (a 2.7σ difference). Note that the expected steepening is determined by the interplay between the energy dependence of the cross section, $\sigma \propto E^{-2}$, and the energy dependence of the scattering angles. Still higher values of $\tau_{\rm sca}$ result in even stronger spectral steepening.

3. DISCUSSION AND CONCLUSIONS

We report here the presence of an extended source around 1E1547.0-5408, which is most likely a PWN. Not counting the spurious (Kaplan et al. 2002) association of a radio nebula with SGR 1806-20 (Kulkarni et al. 1994), this is the first evidence for a PWN around a magnetar. This is of particular interest, as

young PWNe are formed during the whole lifetime of the pulsar, and thus hold a record of the energy released over the lifetime of the pulsars (Pacini & Salvati 1973; van der Swaluw & Wu 2001; Chevalier 2004). This is important for magnetars, because according to one theory magnetars are born with rapid initial spin periods ($P_i \lesssim 3$ ms; Duncan & Thompson 1992, 1996), a theory that was recently challenged on observational grounds (Ferrario & Wickramasinghe 2006; Vink & Kuiper 2006). But even if initial periods shorter than 3 ms seem unlikely, a little is known about the initial spin periods of magnetars. The presence of a PWN may therefore cast new light on this issue, as it may provide evidence that the initial spin period was much shorter than the present spin period.

In addition, the PWN around 1E1547.0-5408 may provide new insight into the connection between AXP/SGRs and other young pulsars that have slightly lower magnetic fields (McLaughlin et al. 2003; Kaspi & McLaughlin 2005), and that do not have all the magnetar characteristics. A recent AXP-like burst from the rotation powered pulsar PSR J1846-0258 already suggests that there is a continuum in properties from pulsars with average magnetic fields of 10^{12} G to magnetars (Gavriil et al. 2008). PSR J1846-0258 has an inferred surface magnetic field of 4.9×10^{13} G and is surrounded by a PWN and a SNR shell, Kes 75 (Kargaltsev & Pavlov 2008). Another pulsar with a relatively high surface magnetic field ($B = 4 \times 10^{13}$ G), PSR J1119-6127, is also surrounded by a PWN, which appears jet-like in morphology (Safi-Harb & Kumar 2008). A third case of a high magnetic field pulsar with a PWN, RRAT J1819-1448, was recently reported by Rea et al. (2009).

One problem in interpreting the presence of a PWN around a magnetar is that we do not a priori know whether the PWN is powered by rotational energy loss, as is the case for normal pulsars, or whether the nebula is ultimately powered by the magnetic field of the magnetar. For example, it has been suggested that magnetar magnetospheres are filled with electrons/positrons and/or ions (Thompson et al. 2002), a fraction of which may escape in the form of a relativistic particle wind (Harding 1996; Harding et al. 1999).

A hint that the PWN around 1E1547.0-5408 may be powered by the pulsar spin-down is provided by comparing the ratio of the X-ray luminosity over the spin-down power of the PWN. There is a correlation between the X-ray luminosity and spin-down power of normal young pulsar (Seward & Wang 1988; Verbunt et al. 1996; Cheng et al. 2004), with $\eta_X = L_X/\dot{E}_{\rm rot}$ in the range of 10^{-4}–10^{-2}. Figure 3 shows the correlation as taken from the sample of Cheng et al. (2004). It shows that the PWN around 1E1547.0-5408 is consistent with the general trend, with $\eta \approx 0.01$, although perhaps with a somewhat enhanced X-ray luminosity compared to pulsars with a similar rotational energy loss (at the 1.5σ level). This is unlike the case of RRAT J1819-1448, which has $\eta = 0.2$ (Rea et al. 2009). The value of $\eta \approx 0.01$ for 1E1547.0-5408 is consistent with the idea that its PWN is powered by the pulsar's spin-down. Interestingly, this can be taken as an additional argument against the alternative theory for the behavior of AXP/SGRs namely that they are not magnetars, but neutron stars that have a high spin-down rate due the propeller mechanism (e.g., Marsden et al. 2001).

The idea that the PWN is powered by the pulsar spin-down is also credible given the fact that 1E1547.0-5408 has the largest spin-down power among AXPs/SGRs. If the PWNe around magnetars are powered by magnetic activity, it is not clear why other AXPs/SGRs, some even more active than 1E1547.0-5408, do not show evidence for extended emission. On the other hand,

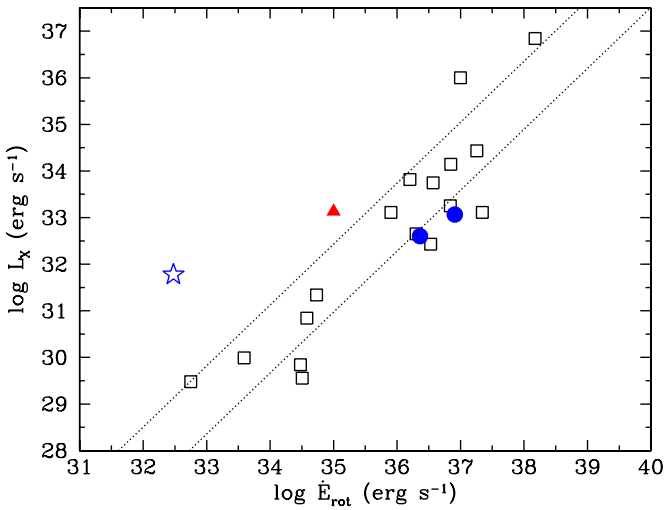

Figure 3. X-ray luminosity, L_X (2–10 keV), and the rotational energy loss, $\dot{E}_{\rm rot}$ of the magnetar 1E1547.0-5408 (filled triangle) compared to the unpulsed X-ray emission of other X-ray pulsars (Cheng et al. 2004). A distance of 9 kpc for 1E1547.0-5408 is assumed (Camilo et al. 2007). The dashed lines indicate the standard deviation around the linear regression relation between $\dot{E}_{\rm rot}$ and L_X. Also indicated are the high magnetic field pulsars PSR J1846-0258 (Kargaltsev & Pavlov 2008; Gavriil et al. 2008) and PSR J1119-6127 (Safi-Harb & Kumar 2008) with filled circles, and RRAT J1819-1458 (Rea et al. 2009) with a star-like symbol.

it is not quite clear why the X-ray spectrum of the PWN is rather steep, $\Gamma \approx -3.5$, compared to PWNe around ordinary pulsars, which have $\Gamma \approx -2$ (Kargaltsev & Pavlov 2008). This may be taken as a hint for another origin, but it may also be explained by the much faster spin evolution of a magnetar compared to other young pulsars. Using the terminology of Pacini & Salvati (1973), most young PWNe are in phase 2 of their evolution, i.e., the pulsar has been a more or less constant source of relativistic particles. In that case, the spectral index beyond the synchrotron break is steeper by only $\Delta\Gamma = 0.5$ compared to the radio spectral index. The PWN around 1E1547.0-5408 is most likely in phase 3: its spin-down luminosity has been rapidly decreasing during its short life ($\tau_{\rm char} \sim 1400$ years). This means that the average age of the relativistic electron populations is skewed toward the total age of the PWN. However, this does not necessarily lead to a steeper spectrum (e.g., Pacini & Salvati 1973). This is an aspect of the nebula around 1E1547.0-5408 that needs further clarification.

Finally, we emphasize that our discovery is based on a *Chandra* observation of only 9.6 ks. A much deeper observation is likely to reveal further details. For the origin of the PWN, it will be important to know whether there is any substructure that may indicate that the nebula has been created as the result of a discrete number of flares, whether there are jets, or whether it is a more homogeneous source. Deeper observations are also important to obtain better spectra and images of the SNR. This may reveal the nature of its X-ray emission, thermal, or nonthermal, which will help to put better constraints on the age of the SNR. In our view, 1E1547.0-5408 and the extended sources around it may be key objects to understand the origin and evolution of magnetars.

We thank Elisa Costantini for discussions on interstellar dust scattering, and Frank Verbunt for his careful reading of the manuscript. J.V. is supported by a NWO Vidi grant.

REFERENCES

Bock, D. C.-J., Large, M. I., & Sadler, E. M. 1999, AJ, 117, 1578
Camilo, F., Ransom, S. M., Halpern, J. P., & Reynolds, J. 2007, ApJ, 666, L93
Camilo, F., et al. 2006, Nature, 442, 892
Cash, W. 1979, ApJ, 228, 939
Cheng, K. S., Taam, R. E., & Wang, W. 2004, ApJ, 617, 480
Chevalier, R. A. 2004, Adv. Space Res., 33, 456
Draine, B. T. 2003, ApJ, 598, 1026
Duncan, R. C., & Thompson, C. 1992, ApJ, 392, L9
Duncan, R. C., & Thompson, C. 1996, in AIP Conf. Proc. 366, High Velocity Neutron Stars, ed. R. E. Rothschild & R. E. Lingenfelter (Melville, NY: AIP), 111
Durant, M., & van Kerkwijk, M. H. 2006, ApJ, 650, 1070
Esposito, P., et al. 2009, MNRAS, 399, L44
Ferrario, L., & Wickramasinghe, D. 2006, MNRAS, 367, 1323
Gaensler, B. M. 2004, Adv. Space Res., 33, 645
Gavriil, F. P., Gonzalez, M. E., Gotthelf, E. V., Kaspi, V. M., Livingstone, M. A., & Woods, P. M. 2008, Science, 319, 1802
Gavriil, F. P., Kaspi, V. M., & Woods, P. M. 2004, Adv. Space Res., 33, 654
Gelfand, J. D., & Gaensler, B. M. 2007, ApJ, 667, 1111
Gronwall, C., et al. 2008, GCN Circ., 8833, 1
Harding, A. K. 1996, in AIP Conf. Ser. 366, High Velocity Neutron Stars, ed. R. E. Rothschild & R. E. Lingenfelter (Melville, NY: AIP), 118
Harding, A. K., Contopoulos, I., & Kazanas, D. 1999, ApJ, 525, L125
Kaplan, D. L., et al. 2002, ApJ, 564, 935
Kargaltsev, O., & Pavlov, G. G. 2008, in AIP Conf. Ser. 983, 40 Years of Pulsars: Millisecond Pulsars, Magnetars and More, ed. C. Bassa, Z. Wang, A. Cumming, & V. M. Kaspi (Melville, NY: AIP), 171
Kaspi, V. M., & McLaughlin, M. A. 2005, ApJ, 618, L41
Krimm, H. A., et al. 2008a, GCN Circ., 8312, 1
Krimm, H. A., et al. 2008b, GCN Circ., 8311, 1
Kulkarni, S. R., Frail, D. A., Kassim, N. E., Murakami, T., & Vasisht, G. 1994, Nature, 368, 129
Lamb, R. C., & Markert, T. H. 1981, ApJ, 244, 94
Marsden, D., Lingenfelter, R. E., Rothschild, R. E., & Higdon, J. C. 2001, ApJ, 550, 397
McLaughlin, M. A., et al. 2003, ApJ, 591, L135
Mereghetti, S. 2008, A&AR, 15, 225
Pacini, F., & Salvati, M. 1973, ApJ, 186, 249
Predehl, P., & Schmitt, J. H. M. M. 1995, A&A, 293, 889
Rea, N., et al. 2009, ApJ, 703, L41
Safi-Harb, S., & Kumar, H. S. 2008, ApJ, 684, 532
Seward, F. D., & Wang, Z.-R. 1988, ApJ, 332, 199
Smith, R. K. 2008, ApJ, 681, 343
Thompson, C., Lyutikov, M., & Kulkarni, S. R. 2002, ApJ, 574, 332
Tiengo, A., et al. 2009, GCN Circ., 8848, 1
van der Swaluw, E., & Wu, Y. 2001, ApJ, 555, L49
Verbunt, F., et al. 1996, A&A, 311, L9
Vink, J., & Kuiper, L. 2006, MNRAS, 370, L14
Wilms, J., Allen, A., & McCray, R. 2000, ApJ, 542, 914
Woods, P., & Thompson, C. 2006, in Compact Stellar X-ray Sources, ed. W. H. G. Lewin & M. van der Klis (Cambridge: Cambridge Univ. Press)